Dystrophic Dmdmdx rats show early neuronal changes (increased S100β and Tau5) at 8 months, supporting severe dystropathology in this rodent model of Duchenne Muscular Dystrophy

Vidya S Krishnan, L P Thanigaiarasu, R White, Rachael Crew, Thibaut Larcher, Caroline Le Guiner, Miranda D Grounds

▶ **To cite this version:**

Vidya S Krishnan, L P Thanigaiarasu, R White, Rachael Crew, Thibaut Larcher, et al.. Dystrophic Dmdmdx rats show early neuronal changes (increased S100β and Tau5) at 8 months, supporting severe dystropathology in this rodent model of Duchenne Muscular Dystrophy. Molecular and Cellular Neuroscience, 2020, 10.1016/j.mcn.2020.103549 . hal-02932024

HAL Id: hal-02932024
https://hal.inrae.fr/hal-02932024

Submitted on 7 Sep 2020

HAL is a multi-disciplinary open access archive for the deposit and dissemination of scientific research documents, whether they are published or not. The documents may come from teaching and research institutions in France or abroad, or from public or private research centers.

L'archive ouverte pluridisciplinaire **HAL**, est destinée au dépôt et à la diffusion de documents scientifiques de niveau recherche, publiés ou non, émanant des établissements d'enseignement et de recherche français ou étrangers, des laboratoires publics ou privés.

Journal Pre-proof

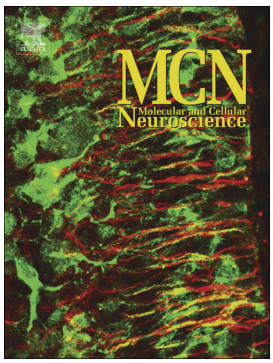

Dystrophic Dmdmdx rats show early neuronal changes (increased S100β and Tau5) at 8 months, supporting severe dystropathology in this rodent model of Duchenne Muscular Dystrophy

V.S. Krishnan, L.P. Thanigaiarasu, R. White, R. Crew, T. Larcher, C. Le Guiner, M.D. Grounds

PII: S1044-7431(20)30172-X

DOI: https://doi.org/10.1016/j.mcn.2020.103549

Reference: YMCNE 103549

To appear in: *Molecular and Cellular Neuroscience*

Received date: 17 July 2020

Revised date: 27 August 2020

Accepted date: 28 August 2020

Please cite this article as: V.S. Krishnan, L.P. Thanigaiarasu, R. White, et al., Dystrophic Dmdmdx rats show early neuronal changes (increased S100β and Tau5) at 8 months, supporting severe dystropathology in this rodent model of Duchenne Muscular Dystrophy, *Molecular and Cellular Neuroscience* (2020), https://doi.org/10.1016/j.mcn.2020.103549

This is a PDF file of an article that has undergone enhancements after acceptance, such as the addition of a cover page and metadata, and formatting for readability, but it is not yet the definitive version of record. This version will undergo additional copyediting, typesetting and review before it is published in its final form, but we are providing this version to give early visibility of the article. Please note that, during the production process, errors may be discovered which could affect the content, and all legal disclaimers that apply to the journal pertain.

© 2020 Published by Elsevier.

Dystrophic *Dmd*^{mdx} rats show early neuronal changes (increased S100β and Tau5) at 8 months, supporting severe dystropathology in this rodent model of Duchenne Muscular Dystrophy

Krishnan VS[1], Thanigaiarasu LP[1], White R[1], Crew R[1], Larcher T[2], Le Guiner C[3], Grounds MD[1]

[1]*School of Human Sciences, the University of Western Australia, Australia, 6009*

[2]*INRAE, Oniris, PAnTher, Nantes, France*

[3]*INSERM UMR1089, University of Nantes, Translational Research for Neuromuscular Diseases, Nantes, France*

Journal Pre-proof

Declaration of competing interest: The authors declare no conflicts of interest related to this work.

Acknowledgments

This research was supported by funding from the Duchenne Parent Project the Netherlands, the Medical and Health Research Infrastructure Fund Western Australia and Torrita (MDG). We thank Erin Lloyd (UWA) for her expert advice on statistical analyses.

ABSTRACT

The intrinsic necrosis of skeletal muscles in animal models of Duchenne muscular dystrophy (DMD) damages neuromuscular junctions (NMJs) with progressively altered NMJs associated with denervation and premature changes in dystrophic nerves. In the *mdx* mouse model of DMD, the proteins S100β and Tau5 are significantly increased in sciatic nerves by 13 months (M) of age, far earlier (by 9M) than in normal wildtype (WT) nerves. Since dystrophic *Dmd*^{mdx} rats are reported to have a more severe dystropathology than *mdx* mice, we hypothesised that *Dmd*^{mdx} rat nerves would show earlier neuronal changes compared with *mdx* nerves. We quantified levels of 8 proteins (by immunoblotting) in sciatic and radial nerves from young adult *Dmd*^{mdx} rats (aged 8M) and *mdx* mice (8M), plus levels of 7 mRNAs (by qPCR) in rat nerves only. Sciatic nerves of 8M *Dmd*^{mdx} rats had more consistently increased levels of S100β and Tau5 proteins, compared with 9M *mdx* mice, supporting pronounced dystropathology in the rat model. There were no differences for mRNA levels, apart from higher gelsolin mRNA in *Dmd*^{mdx} sciatic nerves. The pronounced protein changes in *Dmd*^{mdx} nerves indicate a severe ongoing myonecrosis, and likely consequent myofibre denervation, for the dystrophic rat model. These data support increased neuronal proteins in dystrophic nerves as a novel pre-clinical readout of ongoing myonecrosis for DMD research. In older DMD boys, such progressive neuronal changes over many years are likely to contribute to loss of muscle function, and may complicate evaluation of late-onset clinical therapies.

Keywords: *Dmd*^{mdx} rats, S100β, Tau5, peripheral nerves, *mdx*, Duchenne Muscular Dystrophy

Journal Pre-proof

1 INTRODUCTION

1.1 Dystrophic nerves and persistent myonecrosis in Duchenne muscular dystrophy (DMD)

DMD is a genetic X-linked skeletal muscle wasting disease that affects mainly young boys with severe loss of muscle mass and function within the first decade of life (Verhaart and Aartsma-Rus, 2019). The gene affected in DMD codes for the protein dystrophin that links contractile proteins within myofibres through a transmembrane protein complex to transfer force across the sarcolemma to the extracellular matrix (Petrof et al., 1993). The lack of dystrophin protein results in sarcolemmal fragility and necrosis of dystrophic myofibres (Lapidos et al., 2004; Petrof et al., 1993). The disease process for DMD has been studied intensively in the *mdx* mouse model of DMD (that has equivalent gene defect): while bouts of myonecrosis initially stimulate myogenesis and muscle regeneration, the associated inflammation with increasing fibrosis and desynchronization of myogenesis and regenerative events over time, result in failed new muscle formation and replacement of damaged myofibres with fatty and fibrous connective tissue with consequent severe loss of muscle mass and function in DMD boys (Dadgar et al., 2014; Grounds MD, 2020; Kornegay, 2017). Many studies have focused on the dystrophic skeletal muscles, but recently we described changes in dystrophic nerves of *mdx* mice, with S100β and Tau5 neuronal proteins significantly increased in dystrophic sciatic nerves by 13 months (M) of age (Krishnan et al., 2020). This is far earlier than in normal wildtype (WT) mice where age-related neurodegenerative changes starts to manifest from about 15M-18M of age (Krishnan et al., 2016). In marked contrast with normal ageing, these changes in dystrophic *mdx* nerves result from the key problem of intrinsic persistent myonecrosis that also damages neuromuscular junctions (NMJs).

Early studies in human DMD muscles showed that when the necrotic myofibre segment includes the innervation zone, this will also damage the NMJ and disconnect the necrotic myofibre from its motor nerve supply, with evidence of failure of some nerves to reconnect with the DMD myofibres (Cullen and Mastaglia, 1980). In 1987, changes in dystrophic NMJs were described in *mdx* mice by 6 weeks of age, these were pronounced by 6M and it was concluded that these were secondary to the process of myofibre necrosis and regeneration (Torres and Duchen, 1987). These observations have been widely confirmed by others in *mdx* mice and also dystrophic dogs (Haddix et al., 2018; Marques et al., 2005; Marques et al.,

2007; Torres and Duchen, 1987). It is logical to consider that these early NMJ changes might subsequently impact the nerves that innervate these dystrophic muscles and this was confirmed by our recent study of dystrophic nerves from *mdx* mice aged from 13M up to 18M (Krishnan et al., 2020). These changes in dystrophic nerves suggest irreversible neurodegeneration and represent a secondary longer-term event in the disease progression with likely impaired neuronal function over time, that may become pronounced over many years of ongoing dystropathology in DMD boys and contribute further to the loss of dystrophic muscle function.

1.2 Comparison of dystrophic mouse, dog and rat models for DMD

The *mdx* mouse is a widely used laboratory animal model for DMD, although the disease is mild compared with DMD, likely due to large phenotype differences between the species; this includes the relatively very short growth phase of mice (intensive for 6 weeks postnatal and over by ~3M) compared with humans (about 18 years), the short life span (~2 years for normal mice) and small size of mice (~20-30 gm weight) with far less muscle loading for this quadruped (Grounds, 2008; Willmann et al., 2009) .Many variations of *mdx* mouse models have been explored to try and produce a more severe phenotype that more closely resembles DMD [(reviewed in (van Putten et al., 2020)]. When we compared classic *mdx* mice with D2.*mdx* mice (on a DBA.2 background strain) that were proposed to be a more severe disease model, the surprising lack of change in D2.*mdx* nerves at 13M in contrast with classic *mdx* nerves, did not support severe ongoing myonecrosis and dystropathology in the D2.*mdx* mice (Krishnan et al., 2020). A more severe dystropathology occurs in various strains of dystrophic dogs including the classic Golden retriever muscular dystrophy (GRMD) model that more closely resemble the DMD boys (Kornegay, 2017). The greater growth phase (for about 6M) combined with much larger size and greater muscle loading of dogs and their longer lifespan (compared with rodents), are factors contributing to the pronounced disease severity (Grounds, 2008; Willmann et al., 2009). Unfortunately, GRMD dogs exhibit high individual variability (Kornegay, 2017) and are expensive and difficult to work with, compared with laboratory rodent models.

While normal mice and rats have a similar lifespan of about 2 years, rats have greater growth rate and are about 10 times larger than mice. The *Dmd*^{mdx} rats described in 2014 have a more severe phenotype than *mdx* mice and they die at around 12M of age (Larcher et al., 2014) , well before the 2-year lifespan for normal WT rats. In contrast, *mdx* mice live to at least

about 18 months) (Lefaucheur et al., 1995), with lifespan only slightly shorter than for normal WT mice (Chamberlain et al., 2007). For *Dmd*^{mdx} rat limb skeletal muscles the amount of necrosis is high at 3M but decreased by 7M when there is much fibrosis and adipose tissue with marked loss of muscle strength, and also greater fibrosis and structural remodelling of the heart with altered diastolic function reported (Larcher et al., 2014; Wells, 2018). Since these dystrophic *Dmd*^{mdx} rats appear to have a more severe disease progression than *mdx* mice, they are of much interest for potential use as a research model for DMD (Caudal et al., 2020) although to date there are few additional studies published. Therefore, to test for proposed earlier changes in nerves of *Dmd*^{mdx} rats we analysed sciatic and radial nerves in young adult dystrophic *Dmd*^{mdx} (and WT) rats aged 8M using both protein and RNA quantification, and compared protein levels with nerves of *mdx* (and WT) mice aged 9M.

2 MATERIALS and METHODS

2.1 Animals and tissue collection

Rats: Sciatic and radial peripheral nerves from (hind limbs and forelimbs respectively) of 8M old (aged between 33 and 35 weeks) male Sprague-Dawley control WT rats and dystrophic *Dmd*^{mdx} rats (n=8/for each group) were provided by our French collaborators in Nantes, France (Larcher et al., 2014). These nerves were dissected, snap frozen in liquid nitrogen (left and right nerves separately) and sent to the University of Western Australia in late 2018. The left sciatic and radial nerves were used from each rat for immunoblotting, with a total of 31 nerves being analysed. The right nerves were used for RNA extraction and analysis. It was noted that the frozen sciatic and radial rat nerves (both *Dmd*^{mdx} and WT) had some muscle and connective tissue attached.

Mdx and WT Mice: Peripheral nerves from normal control (WT) C57Bl/10Scsn (n=5) and dystrophic *mdx* male mice (n=8) aged 9M (aged 39 weeks) were sampled for species comparison, as a similar age-related control for the rat study. These mice were aged at the Animal Resources Centre in Western Australia and all experiments were conducted in accordance with the National Health and Medical Research Council (Australia) guidelines approved by the Animal Ethics Committee of the University of Western Australia. Mice were killed by pentobarbital injection followed by cervical dislocation, sciatic and radial nerves dissected carefully away from the surrounding muscles and connective tissues and snap frozen in liquid nitrogen for future protein extraction (Krishnan et al., 2020). Due to the

smaller size of mouse nerves compared with rat nerves, both left and right mouse nerves were pooled for protein extraction (and thus tissue was not available for RNA analyses).

2.2 Protein extraction from nerves and immunoblotting

Protein extraction from the nerves were carried out as described in our previous studies (Krishnan et al., 2020; Krishnan et al., 2016; Krishnan et al., 2017). In short the snap frozen nerves were homogenized in buffer containing 20mM HEPES, 4% (w/v) sodium dodecyl sulphate (SDS) supplemented with protease and phosphatase inhibitor tablets followed by sonication for 10 seconds and centrifugation. After centrifugation, the concentration of the protein in the supernatant was quantified with the *DC*™ protein assay and 10µg of protein/well were resolved on 4-15% (w/v) SDS-PAGE and transferred onto 0.2 µm pore size nitrocellulose membrane using a Trans Turbo Blot system. A common protein sample was loaded on each gel to normalize for detection efficiencies across membranes (Krishnan et al., 2016; Krishnan et al., 2017; Shavlakadze et al., 2013). After transfer, membranes were stained with Ponceau S red stain to visualize the total protein, which was used as a loading control. All primary antibodies used for the proteins analysed by immunoblotting (details in **Table 1**) were diluted (1:1000) in 5% (w/v) BSA (bovine serum albumin) in TBS-T (Tris buffered saline with (0.1% v/v) Tween-20) buffer. The proteins selected for immunoblotting in this study, were based on our recent study in *mdx* mice that showed elevated levels of proteins in dystrophic sciatic nerves at an early age of 13M (Krishnan et al., 2020). After exposure to appropriate horseradish peroxidase (HRP) conjugated secondary immunoblots were developed using Perkin Elmer Western Lightning Ultra (MA, USA) and the chemiluminescent signal was captured using a ChemiDoc MP Imaging System (Bio-Rad, NSW, Australia). Resultant images were quantified using ImageJ software by normalizing bands to the respective total protein stained with Ponceau S red stain in the same gel (Krishnan et al., 2020).

Table 1. Primary antibodies used for immunoblotting rat and mouse sciatic and radial nerves

Host	Antigen	Source & number	Function	Reference
Mouse	S100β	Sigma Aldrich; S-2532, Australia	Protein marker for Schwann cells in PNS	(Duobles et al., 2008)
Mouse	Tau5	Biosource Int. AHB0042, USA	Microtubule associated protein that stabilizes microtubule assembly in axons	(Lee and Rook, 1992)
Rabbit	Gelsolin	Cell Signalling; 12953, USA	Protein that binds actin, high in myelin forming cells	(Tanaka and Sobue, 1994)
Rabbit	Vimentin	Cell Signalling; 5741, USA	Intermediate filament that regulates PNS myelination	(Triolo et al., 2012)
Mouse	SMI-32	Covance; SMI-32R	Heavy neurofilament protein that maintains axon calibre	(Yuan et al., 2012)
Goat	ChAT	Chemicon; AB144P, USA	Enzyme responsible for synthesis of acetylcholine	(Dobransky and Rylett, 2003)
Rabbit	p62	Cell Signalling, 5114, USA	Protein that binds ubiquitin and is involved in autophagy	(Myeku and Figueiredo-Pereira, 2011)
Mouse	APP-clone 22C11	Millipore MAB348	Synaptic development and function	(Caldwell et al., 2013)

2.3 RNA extraction from peripheral nerves of 8M Dmd^{mdx} and WT rats and qPCR analysis

Seven genes selected for RT-qPCR gene expression analysis of the rat sciatic and radial nerves (n=8/group) are summarised in **Table 2**. These genes were selected on the basis that nuclei of Schwann cells, fibroblasts and others interstitial cells associated with neurons express their mRNAs. The situation is more complex in long mature axons; while many mRNAs are located near the nucleus in the axonal cell body in the spinal cord, it is now recognised that there is a subcellular repertoire of mRNAs in axons associated with motor proteins carrying transcripts as messenger ribonucleoprotein (mRNP) complexes along microtubules down to potential growth cones and pre-synaptic terminals (Gumy et al., 2014). However, the situation seems unclear for mature axons in intact peripheral nerves *in vivo*, especially for the mid-region of the long sciatic nerve as sampled in this study.

The 7 mRNAs analysed were S100 calcium binding protein beta (*S100ß)* expressed mainly in Schwann cells, gelsolin (*Gsn)* in Schwann cells, collagen type 1 alpha 1 (*Col1a1*) in axons required for Schwann cell function, myelin basic protein (*Mbp)* in Schwann cells, nerve growth factor receptor (*Ngfr*) also known as P75NR in Schwann cells and perhaps fibroblasts and endothelial cells of blood vessels, microtubule-associated protein tau (*Mapt*) in axons, and brain-derived neurotrophic factor (*Bdnf*) in Schwann cells and possibly other cells. Total RNA was extracted from nerves using the TRIzol method (Invitrogen), according to the manufacturer's instructions. Quality and concentration of RNA was determined spectrophotometrically (Nanodrop ND-1000) and 1µg of RNA was reverse transcribed to cDNA using a QuantiTect Reverse Transcription Kit (Qiagen). The relative mRNA expression was analysed via real-time qPCR on the Rotor-Gene Q system. All primers (**Table 2**) were purchased as QuantiTect primer assays, apart from the reference genes peptidylprolyl isomerase A *(Ppia*) and tyrosine 3-monooxygenase/tryptophan 5-monooxygenase activation protein zeta (*Ywhaz*), which were designed using Primer-BLAST (http://www.ncbi.nlm.nih.gov). Standard curves were generated from 10-fold serial dilutions of gel extracted PCR product and relative gene expression was determined using Q-Rex software. All samples were run in duplicate and standardised against *Ppia* and *Ywhaz* using the GeNorm algorithm (Vandesompele et al., 2002)

Gene	**Qiagen name or Primer sequence**	**Catalogue No. or T_a (°C)**
S100 beta	S100b.	QT00184744
Gsn	Gelsolin	QT01615124
Col1a1	Col1a1	QT01081059
Mbp	Mbp	QT00199255
Ngfr	Ngfr	QT00181874
Mapt	Mapt	QT00174797
Bdnf	Bdnf	QT00375998
Ppia	F 5'- AGCATACAGGTCCTGGCATC-3' R 5'- TTCACCTTCCCAAAGACCAC -3'	62 62
Ywhaz	F 5' GACGGAGCTGAGGGACATCTGC 3' R 5' GGCTGCGAAGCATTGGGGATCA 3'	60 60

Table 2. Genes analysed for qPCR (Qiagen) with 2 reference genes

2.4 Statistical analysis

GraphPad Prism version 8.0.1 was used as the statistical package.

For the 8M WT and *Dmd*^{mdx} rats, the protein data from immunoblotting for the (left) sciatic and radial nerves were analysed separately using 2-tailed unpaired Student's t-test, whereas mRNA levels by qPCR were analysed by the Mann Whitney test separately for (right) rat sciatic and radial nerves. For both, the significance threshold was set at $p \leq 0.05$. To determine whether there is an overall strain or nerve effect for each protein/mRNA tested, a 2-way-ANOVA followed by Fischer's Least Significant Difference (LSD) tests was conducted and a Bonferroni corrected $p \leq 0.0083$ was considered as significant.

Similarly (as done for the rats), protein data for the sciatic and radial nerves of the 9M WT and *mdx* mice were analysed separately using 2-tailed unpaired Student's t-test with significance threshold set at $p<0.05$. To evaluate an overall strain or nerve effect for each protein, a 2-way-ANOVA followed by Fischer's Least Significant Difference (LSD) tests was conducted, with a Bonferroni corrected $p \leq 0.0083$ considered as significant.

A direct species comparison between *Dmd*^{mdx} rats and *mdx* mice was not done, as samples for each species were run on different gels.

4 RESULTS

4.1 Protein quantification by immunoblotting of rat and mouse sciatic and radial nerves.

The selection of proteins for immunoblotting used this study (detailed in **Table 1**) was based on our recent study which showed significantly increased levels of S100β and Tau5 in *mdx* sciatic nerves by 13M of age (Krishnan et al., 2020).

S100β. In the 8M rats, S100β protein levels were significantly higher (by ~40%) in dystrophic sciatic nerves of *Dmd*^{mdx}, compared with WT, rats (p=0.0101, unpaired t-test) (**Figure 1a, d)** although there was no significance difference for radial nerves between the strains. An overall strain effect was observed (p=0.0229, 2-way-ANOVA), suggesting higher protein levels in the *Dmd*^{mdx} rat nerves.

Similarly in mice, S100β levels in the *mdx* sciatic nerves were ~40% greater than that in the WT sciatic nerves (p=0.0393, unpaired t-test) **(Figure 1f, i**) with no strain difference for the radial nerves. An overall strain effect was observed (p=0.0134, 2-way-ANOVA), suggesting increased S100β levels in the *mdx* nerves.

Tau5. In *Dmd*^{mdx} sciatic nerves there was a 30-40% increase in Tau5 protein, compared with WT rat nerves ($p<0.001$, unpaired t-test) (**Figure 1b, e,)** with no significant strain difference for radial nerves.

In contrast, in mice there were no significant differences in Tau5 protein levels between strains for the sciatic nor the radial nerves (**Figure 1g, j)**: however, an overall strain effect was seen in Tau5 protein levels ($p=0.0410$, 2-way-ANOVA), suggesting higher levels in the *mdx* compared with WT nerves.

Data variation between samples for mdx mice aged 9 months for S100β and Tau5. There appeared to be high data variation between nerves of individual *mdx* mice compared with *Dmd*^{mdx} rats for S100β and Tau5 (and with the WT strains). To investigate this further, *mdx* mice were identified as either 'low' or 'high' individuals, the 'low' and 'high' groups were categorised based on S100β protein values in sciatic nerves of each individual *mdx* mouse, and divided into 2 groups (n=4/group), with the same 2 groups compared for data distribution for all proteins. The same exercise was done for the *Dmd*^{mdx} rats (n=4/group). A comparison for the 2 groups within each dystrophic species is shown for S100β and Tau5 in *Dmd*^{mdx} rat and *mdx* nerves in **Figure 2**. For *Dmd*^{mdx} nerves only S100β protein levels in sciatic nerves showed significant differences between the 2 groups, with no marked variation for Tau5 protein levels nor radial nerves **(Figure 2a, b)**. In marked contrast, in *mdx* nerves there were significant differences between the groups for levels of both S100β and Tau5, in both the sciatic and radial nerves **(Figure 2c, d),** demonstrating high individual variation. This suggests that pronounced changes in these 2 key neuronal proteins may be starting to become evident around 9M of age for about half this population of *mdx* mice; whereas these changes for both S100β and Tau5 are more well established in the dystrophic rats by 8M (**Figures 1** and **2**). As the samples were initially analysed using 3 gels/species, to rule out the possibility of inconsistensies (between these 3 gelss), the samples for each species were subsequently loaded onto a single big 26 well SDS gel and quantified, with a separate gel for all sciatic and radial nerve samples (**Supplementary Figure 1)**. Consistent results were obtained between samples run on the small and large gels , with the exception of S100β levels in radial nerves of *Dmd*^{mdx} rats that then showed a significant increase on the large gel ($p=0.0126$) (**Supplementary Figure 1i)**.

Gelsolin. For the rats, no change in gelsolin levels was observed between the two strains for both the sciatic and radial nerves (**Figure 3a, c**), and there was no overall strain or nerve

effect. For mice, an overall nerve effect was observed in gelsolin levels (p=0.0008) with a ~44% decrease in the WT radial nerves when compared with WT sciatic (p=0.0011 by 2-way-ANOVA) **(Supplementary Figure 2a, e**)

The comparison of protein levels for the 2 subgroups of dystrophic rats and mice for gelsolin (and all other proteins below) are shown in **Supplementary Figures 3** and **4**, respectively, and discussed at the end of this section**.**

Vimentin. In rat sciatic nerves, no changes in vimentin protein levels were observed between the strains, although vimentin protein was significantly increased in *Dmd*^{mdx} radial nerves compared with WT **(Figure 3d, f**) (p=0.0165, unpaired t-test). There was an overall strain effect, with a trend for higher vimentin protein in the *Dmd*^{mdx} nerves (p=0.0396, 2-way-ANOVA). For mice, no overall strain or nerve effects for vimentin levels were observed **(Supplementary Figure 2b, f**).

SMI-32. For rats, no overall strain or nerve effects were observed for SMI-32 protein levels (**Figure 3g, i).** For mice, there was no change in SMI-32 levels between the two strains for both the sciatic and radial nerves although a nerve effect was seen (p<0.0001, 2-way ANOVA with increased SMI-32 protein levels in the sciatic nerves of both WT (p=0.0082) and *mdx* (p<0.001) mice compared with radial nerves (**Supplementary Figure 2c, g**).

ChAT. For rats, there were no changes in ChAT levels between the two strains for both the sciatic and radial nerves and no overall strain or nerve effect (**Figure 4a, c**). In mice, there was no difference between the two strains for ChAT protein levels in sciatic nor the radial nerve (**Supplementary Figure 2h, l**). However**,** an overall nerve effect was observed (p<0.001) with decreased ChAT protein levels in the WT radial nerves when compared with WT sciatic nerves (p=0.0013).

p62. For rats, there were no significant differences in levels of p62 protein between the strains for both sciatic and radial nerves: however, there was an overall nerve effect (p=0.0100, 2-way-ANOVA), suggestive of increased protein levels in the sciatic nerves for both WT and *Dmd*^{mdx} rats (**Figure 4d, f**). For mice, no overall strain nor nerve effects were observed for p62 protein levels (**Supplementary Figure 2i, m).**

APP. For rats, there were no changes in APP levels between the two strains for both the sciatic and radial nerves and no overall strain or nerve effect (**Figure 4g, i**). In mice, there

was an overall nerve effect for APP protein ($p<0.0001$, 2 way-ANOVA) with a ~44% decrease in levels in the WT radial compared with WT sciatic nerves ($p<0.001$) (**see Supplementary Figure 2j, n).**

The comparison of subgroups of dystrophic rats and mice for the proteins gelsolin, vimentin, SMI-32, ChAT, P62 and APP (**Supplementary Figures 3** and **4**) showed no difference in any proteins for sciatic nerves, but some variation for radial nerves. Significant difference between the 2 groups for dystrophic rat radial nerves were seen for the proteins gelsolin, p62 and APP (**Supplementary Figure 3**), and for *mdx* mice for gelsolin and vimentin (**Supplementary Figure 4)**. Since comparison of the full groups of WT and dystrophic nerves showed no significant strain difference, with the exception of vimentin (**Figure 3**), for all of these proteins for both rats and mice (**Figure 4** and **Supplementary Figure 2**), these variations for other proteins within the groups of dystrophic nerves were not considered of overall importance and therefore were not discussed further.

4.2 Gene expression analysis by qPCR in Dmd^{mdx} rat nerves.

Levels of mRNAs in the (right) sciatic and radial nerves were analysed by qPCR for 7 genes including *S100β*, *Mapt*, *Gsn1*, *Col1a1*, *Mbp*, *Ngfr1/p75* and *Bdnf*. Levels of mRNA were similar for most genes between the WT and *Dmd*^{mdx} rat sciatic and radial nerves (**Figure 5**): the exception was for gelsolin mRNA that was significantly increased in sciatic nerves of Dmd^{mdx} compared with WT rats ($p=0.0499$) (**Figure 5b**), with no changes in radial nerves. For *Mapt,* the mRNA levels were below limits of detection and hence could not be analysed (as anticipated since this is likely an axonal protein and most RNA appears to be translated into protein near the mature axon nucleus in the spinal cord)

5. DISCUSSION

It is emphasised that disturbances to the intact mature dystrophic (DMD) nerves are presumed to occur in response to altered neuronal connections at the level of NMJs in the distant target myofibres, as a result of repeated bouts of intrinsic necrosis in dystrophic skeletal muscles throughput the body (indicated in **Figure 6**), with likely sprouting of the distal nerve endings in attempts to reinnervate the altered (denervated) NMJs and dystrophic myofibres (see Introduction; Haddix et al., 2018). This slowly progressive dystrophic situation that heterogeneously affects nerves *in vivo*, does not readily relate to the many studies of normal nerves as tissue cultured neurons, or to *in vivo* studies that identify patterns

of gene expression during peripheral nerve embryogenesis and development, or in response to acute experimental homogeneous nerve injury or denervation. However, heterogeneous changes in individual nerves do occur during normal ageing and are closely associated with age-related loss of skeletal muscle mass and function (sarcopenia) (Krishnan et al, 2016). Sarcopenia (that manifests in hind-limbs of normal rodents from about 15 to 18M of age) is associated with increased expression in myofibres of genes indicating denervation, with heterogeneous changes in NMJs (indicating denervation), altered proteins and mRNA in hind-limb peripheral neurons (Pannerec et al., 2016) and central changes to motor neurons in the spinal cord (Krishnan et al., 2018). These linked age-related events occur in a similar timeline (in the absence of any marked necrosis of healthy ageing muscles), although which components of the neuromuscular system drive sarcopenia remain unclear.

The study of proteins and RNA levels in dystrophic nerves from male *Dmd*^{mdx} rats aged 8M, (compared with WT), revealed significantly increased levels of S100β and Tau5 proteins and increased mRNA for gelsolin in the *Dmd*^{mdx} rat sciatic nerves, plus increased S100β (**Supplementary Figure 1f, i**) and vimentin proteins in the radial nerves of *Dmd*^{mdx} rats. These observations indicate that these changes in dystrophic nerves of *Dmd*^{mdx} rats start before 8M. These new neuronal data strongly indicate that there is significant ongoing myonecrosis in *Dmd*^{mdx} rats, associated with well-established fibrosis from 7 months, and support the proposal of a severe dystropathology in this rat model of DMD (Larcher et al., 2014). Our previous studies using 2 strains of *mdx* mice, showed no changes in levels of these neuronal proteins in D2.*mdx* nerves aged 9 nor 13M, although protein levels of both S100β and Tau5 were increased for nerves of classic *mdx* mice at 13M; indicating a more severe ongoing myonecrosis phenotype for the *mdx* mice, compared with D2.*mdx* mice (Krishnan et al., 2020). Since the original study did not include *mdx* mice at 9M, this younger age group of *mdx* mice (9M) was selected for comparison with the *Dmd*^{mdx} rats aged 8M in the present study. While S100β protein was significantly increased in *mdx* nerves at 9M, compared with WT (**Figure 1**), this seemed to be pronounced for only about 50% of the *mdx* mice and this was also the case for Tau5 protein (**Figure 2**), suggesting that these neuronal changes were not yet fully manifesting in all *mdx* mice at 9M. This contrasts with the one month younger *Dmd*^{mdx} rats (8M) where the neuronal proteins S100β and Tau5 were more reliably elevated, especially in sciatic nerves. Overall, these data strongly support the *Dmd*^{mdx} rats as a consistent and severe rodent model for pre-clinical studies.

These increased neuronal (S100β and Tau5) proteins in *Dmd*^{mdx} rat sciatic nerves by 8M provide a useful readout of cumulative irreversible damage resulting from ongoing myonecrosis. These progressive neuronal changes indicate neurodegeneration that may be irreversible and likely result from progressive denervation of dystrophic muscles: it is noted that advanced myofibre denervation may account for elevated dystrophin protein observed in myofibres of older DMD boys (discussed in (Krishnan et al., 2020)). These new rat data endorse increased S100β and Tau5 proteins in dystrophic nerves as useful new biomarkers for pre-clinical studies (using mammalian animal models of DMD) to monitor the long-term efficacy of therapies that aim to reduce myonecrosis e.g. molecular/genetic interventions to restore dystrophin protein, or drugs/nutripharmaceuticals to protect myofibres. Further discussion of the protein and RNA changes in dystrophic nerves and their significance in the *Dmd*^{mdx} rat is provided below.

5.1 Increased S100β protein in Dmd*^{mdx} *rat (and mdx) nerves, linked to Schwann cells.

These new data for the younger rodents showed significantly increased levels of S100β protein in sciatic and radial nerves of *Dmd*^{mdx} rats aged 8M (compared with WT nerves). For the *mdx* mice aged 9M, increased S100β protein was initially evident only in the sciatic, but not radial nerves: due to high variability the *mdx* mice were split two groups (n=4 mice/group) and then S100β protein was seen to be significantly increased for the 'high' group compared with the 'low' group for both the *mdx* sciatic and radial nerves at 9M (**Figure 2**). Our previous study of dystrophic nerves from *mdx* aged 13, 15 and 18M (Krishnan et al., 2020) showed consistently higher S100β protein in sciatic nerves at all ages (compared with WT), with no changes for radial nerves (although groups were smaller with only n=4-6 mice/group). Increased S100β protein in nerves indicates some disturbance of Schwann cell activity possibly associated with sprouting at the damaged dystrophic NMJ, or perhaps protein accumulation due to impaired autophagy, as discussed in our previous study of older *mdx* mice (Krishnan et al., 2020). In NMJs of the *mdx* mouse and also the GRMD dog, sprouting and nerve terminal branching (which reflects the fragmented distribution of AChRs) is evident from 2M to >1 year of age (Haddix et al., 2018; Lyons and Slater, 1991; Minatel et al., 2003; Pratt et al., 2015) and this fragmented pattern becomes more pronounced in older dystrophic NMJs (Haddix et al., 2018). Axonal sprouting and the formation of new endplates was also observed at the NMJs from 13 boys with DMD, aged 4-14 years (Harriman, 1976). The increased S100β levels in our study is consistent with such sprouting at the dystrophic nerve terminals (that may affect Schwann cells throughout the length of the

nerve). Increased S100β levels with impaired protein turnover were implicated in progressive neurodegeneration in ageing normal mice (Krishnan et al., 2016) and in older mouse peripheral nerves Schwann cell plasticity and myelin clearance were reduced (Painter et al., 2014). Since NMJ remodelling has been observed in the DMD animal models and patients at early ages, it seems likely that subtle neurodegenerative changes have started to occur in the Schwann cells by 8M and 9M in the dystrophic rat and mouse nerves respectively.

The mRNA analyses did not show any altered expression of S100β in *Dmd*^{mdx} rat sciatic nor radial nerves, suggesting that the increased S100β protein may not be due to increased protein synthesis. Instead, the elevated S100β protein might be accounted for by protein accumulation due to delayed turnover. Protein accumulation is implicated in ageing normal nerves where p62 protein levels (a marker for impaired autophagy that can lead to protein accumulation) were significantly increased by 22M (Krishnan et al., 2016); however, p62 protein levels were not increased in the *Dmd*^{mdx} rat nerves at 8M. Further studies are required to elucidate this situation.

In the context of Schwann cell changes, gelsolin was also measured, as this is expressed in many cell types including Schwann cells and is required for the timely re-myelination of the sciatic nerve following experimental injury (Goncalves et al., 2010; Tanaka and Sobue, 1994). Gelsolin protein levels showed no changes for dystrophic nerves, consistent with our recent studies in older *mdx* mice between 15-18M of age (Krishnan et al., 2020). Thus unaltered protein levels for gelsolin do not correspond with the increased S100β in dystrophic *Dmd*^{mdx} rat and *mdx* nerves by 8M and 9M. However, the mRNA for gelsolin was significantly higher in the 8M *Dmd*^{mdx} rat sciatic, but not radial nerves (compared with WT); since this elevated mRNA does not fit with the unaltered gelsolin protein levels in the *Dmd*^{mdx} rat sciatic nerve, the implications are not clear.

Vimentin, the intermediate filament protein in cytoskeleton of Schwann cells and many cell types (Triolo et al., 2012) was also measured in the context of Schwann cell changes. Vimentin expression is usually high during embryonic development; whereas postnatal vimentin expression is restricted to myelin-forming Schwann cells (Jessen and Mirsky, 1991) and expression is upregulated following nerve injury (Triolo et al., 2012). In *Dmd*^{mdx} rat nerves, vimentin protein was significantly increased in radial, but not sciatic nerves (compared with WT), and there was an overall trend for higher vimentin protein in the *Dmd*^{mdx} nerves. No differences in vimentin protein levels were observed for the *mdx* nerves at

9M. The rat data support some possible disturbance related to Schwann cells, but might also reflect increased fibrosis in the *Dmd*^{mdx} rat nerves (since interstitial fibrosis is also pronounced in *Dmd*^{mdx} rat hearts (Larcher et al., 2014). The explanation of fibrosis is also supported by our prior study (Krishnan et al., 2020) where *mdx* sciatic nerves also had no increase in vimentin at 13 nor 15M of age (compared with WT), yet for the D2.*mdx* mice that are characterised by intrinsic high levels of fibrosis, vimentin was significantly elevated by 9M in D2.*mdx* sciatic nerves (and was higher than *mdx* nerves at 13M), yet S100β protein was unchanged in these D2.*mdx* nerves: hence high fibrosis was the logical explanation.

After experimental nerve transection in normal rats, detailed long term studies of the denervated muscles show a marked increase in fibrosis that accumulates over time (Lu et al., 1997) and also a decrease in numbers of capillaries and hence blood supply (Carlson, 2014): both of these consequences of myofibre denervation would be expected to exacerbate disease severity in later stages of DMD. However, they are unlikely to become conspicuous in dystrophic rodent muscles due to the relatively very short growth phase and short life span of < 2 years for *Dmd*^{mdx}rats, compared with decades for DMD boys.

5.2 Increased Tau5 protein in Dmd^{mdx} *rat (and mdx) nerves*

Tau5 promotes microtubule assembly and stabilization and plays a major role in maintaining the normal morphology of axons (Lee and Rook, 1992) with abnormal phosphorylation and aggregation of tau proteins implicated in many neurodegenerative disorder (Avila, 2006). Tau5 protein was significantly increased in *Dmd*^{mdx} rat sciatic, but not radial, nerves at 8M (compared with WT). While Tau5 protein was not initially increased for the *mdx* sciatic nor radial nerves, when the *mdx* mice were separated into a 'low and a 'high' group (n=4 mice/group) and the 2 groups compared, Tau5 protein was significantly increased for the 'high' half of the *mdx* sciatic and radial nerves at 9M. The same individual *mdx* mice with the high Tau5 values, also had high S100β values (see **Figure 2**), indicating that only about half the *mdx* mice were manifesting neuronal changes at 9M of age, and that the remainder had not yet reached this stage. In our previous *mdx* nerve study, Tau5 was significantly increased in sciatic nerves by 13M with further increases up to 18M of age, and in radial nerves was also increased by 18M (Krishnan et al., 2020). This early increase in Tau5 protein in dystrophic nerves may reflect various changes in the axons over time, but initially might be due to increased axonal transport to deliver more neurotransmitter to the progressively damaged NMJ. It is well documented that both pre- and postsynaptic structural abnormalities contribute to deficits in *mdx* NMJ function (Pratt et al., 2015) and that NMJs becomes more

fragmented with age (Haddix et al., 2018). Plus electrophysiological studies in dystrophic *mdx* mice show that in response to the postsynaptic sensitivity loss for the neurotransmitter acetylcholine (ACh), there was a compensatory increase in the number of ACh quanta released from the pre-synaptic nerve terminal per nerve impulse (van der Pijl et al., 2016). Whether this altered NMJ transmission reflects increased axonal transport of AchR to the nerve endings (possibly reflecting increased Tau5 protein), or altered recycling of the synaptic vesicles (Sheard et al., 2010) is not known.

5.3 Comparison with other dystrophic nerves

While we measured protein levels in dystrophic nerves that innervate limb skeletal muscles, a recent study using electron microscopy describes striking pathological changes in phrenic and hypoglossal (XII) nerves of *mdx* mice (n=3) aged 12 months (Dhindsa et al., 2020), with severe axonal demyelination and mitochondrial abnormalities that were pronounced for large calibre axons, and it was concluded that this degeneration was initiated at the NMJ. The phrenic is the only source of motor innervation to the diaphragm and thus plays a crucial role in breathing, and the hypoglossal XII provides motor control for most muscles of the tongue. It is widely recognised that the diaphragm is the most severely affected muscle in the *mdx* mouse, due in large part to its obligatory ceaseless workload, with marked loss of muscle and replacement by fibrous connective tissue, and respiratory failure is the most common cause of death in DMD (Chamberlain et al., 2007; Stedman et al., 1991). Another severely affected *mdx* skeletal muscle is the tongue that, surprisingly, has barely been studied (Chamberlain et al., 2007; Lefaucheur et al., 1995) yet dysphagia (difficulty in swallowing) is widely reported in DMD boys (Toussaint et al., 2016). Thus both of these nerves are of much clinical relevance for DMD. It would be interesting to quantify S100β and Tau5 proteins levels in these nerves and to study them further at earlier (and later) time points and in the more severe animal models of DMD.

CONCLUSIONS

Since 2014, few descriptive studies have been carried out on the promising dystrophic *Dmd*^{mdx} rat model for DMD (Larcher et al., 2014) and these new data further support the severe ongoing progressive disease pathology and sustained myonecrosis in the dystrophic rat muscles, that appears to be more severe than for *mdx* mice. These neuronal data endorse the *Dmd*^{mdx} rat as an excellent pre-clinical rodent model for DMD. The neuronal changes were consistently evident by 8M of age (with S100β and Tau5 proteins both increased in sciatic

nerves) compared with the *mdx* mice aged 9M. The confirmation of these neuronal changes in the 8M *Dmd*^{mdx} rats, combined with data now for *mdx* mice aged 9M (as well as previous nerve data for 13M-18M old *mdx* mice), validates the use of these new neuronal markers as a useful indirect pre-clinical readout (using immunoblotting) to monitor the extent of ongoing myonecrosis in dystrophic muscles. Clearly more pre-clinical studies are required to provide detailed information, to clarify the reasons and implications, the earliest manifestation and later consequences of these neuronal changes, including the extent to which spinal cord connectivity (Krishnan et al., 2018) may show alterations at much older ages. It seems especially important to extend these neuronal studies to GRMD (and other dog) models of DMD where the disease manifestation is more pronounced: this reflects the relatively greater length of the growth phase (associated with pronounced myonecrosis), much bigger overall size (affecting muscle loading), and the much longer life span of dystrophic dogs (allowing more time for manifestation of secondary progressive neuronal changes), compared with rodents. Further studies are required to better understand the likely progressive irreversible neuronal alterations in DMD over time with major implications for loss of contractile function, especially important to consider for therapies planned for older DMD patients. These neuronal readouts provide a new pre-clinical biomarker to help measure long-term benefits of therapies that aim to protect dystrophic muscles from myonecrosis, especially relevant to studies of molecular and gene therapies that aim to replace dystrophin.

Figure legends

Figure1. S100β and Tau5 protein quantification in sciatic and radial nerves from male normal WT and dystrophic *Dmd*^{mdx} rats aged 8M and *mdx* mice aged 9M. Bands immunoreactive to S100β (**a, f**) and Tau5 (**b, g**) were normalised to the respective lanes of total protein (**c, h**) visualized with Ponceau S red. All data are mean ± SEM. Individual data points on histograms indicate each animal in the group (shown by white dots with black border). Data (**d, e, i and j**) analysed separately by unpaired t-tests; *P ≤ 0.05, ***P≤0.001. Y-axis represents arbitrary units.

Figure 2. **Comparison of 'low' and 'high' groups of protein samples** (n=4/group) for S100β (**a, c**) and Tau5 (**b, d**) in sciatic and radial nerves from male *Dmd*^{mdx} rats aged 8M and *mdx* mice aged 9M. All data are mean ± SEM by unpaired t-tests. Individual data points on histograms indicate each animal in the group (shown by white dots with black border). *P ≤ 0.05, **P≤0.01, ***P≤0.001. Y-axis represents arbitrary units.

Figure 3. **Gelsolin, vimentin and SMI-32 protein quantification** in sciatic and radial nerves from male WT and *Dmd*^{mdx} rats aged 8M. Bands immunoreactive to gelsolin (**a),** vimentin **(d)** and SMI-32 **(g)** were normalised to the respective lanes of total protein (**b, e, h**) visualized with Ponceau S red. All data are mean ± SEM. Data (**c, f, i**) analysed separately by unpaired T-tests. Individual data points on histograms indicate each animal in the group (shown by white dots with black border). Y-axis represents arbitrary units.

Figure 4. **ChAT, p62 and APP protein quantification** in sciatic and radial nerves from male WT and *Dmd*^{mdx} rats aged 8M. Bands immunoreactive to ChAT (**a),** p62 **(d)** and APP **(g)** were normalised to the respective lanes of total protein (**b, e, h**) visualized with Ponceau S red: All data are mean ± SEM. Data (**c, f, i**) analysed separately by unpaired T-tests. Individual data points on histograms indicate each animal in the group (shown by white dots with black border). Y-axis represents arbitrary units.

Figure 5. **Gene expression analyses by qPCR** for *S100β*, Gelsolin (*Gsn*), Collagen 1(*Col1a1*), *Mbp*, *Ngfr1/p75* and *Bdnf* for male WT and *Dmd*^{mdx} rats aged 8M. Data (**a-f**) analysed separately by unpaired T-tests. *$P \leq 0.05$. Individual data points on histograms indicate each animal in the group (shown by white dots with black border). Y-axis represents arbitrary units.

Figure 6. Schematic diagram of the sequence of events causing progressive changes in dystrophic nerves of a DMD boy. This indicates the links between the primary event of (**1**) repeated intrinsic necrosis of most skeletal muscles throughout the body and consequent secondary events of (**2**) morphologically altered and denervated NMJs, leading to (**3**) progressive changes over time in dystrophic nerves: shown here for muscle in leg and associated sciatic nerve with high power (HP) view of NMJs and motorneuron. This study analysed dystrophic nerves from 2 rodent models of DMD, comparing adult dystrophic *Dmd*^{mdx} rats with classic *mdx* mice: shown here for comparison of scale with young DMD boy.

Journal Pre-proof

6. REFERENCES

Avila, J., 2006. Tau phosphorylation and aggregation in Alzheimer's disease pathology. FEBS letters 580, 2922-2927.

Caldwell, J.H., Klevanski, M., Saar, M., Muller, U.C., 2013. Roles of the amyloid precursor protein family in the peripheral nervous system. Mech Dev 130, 433-446.

Carlson, B.M., 2014. The Biology of Long-Term Denervated Skeletal Muscle. Eur J Transl Myol 24, 3293.

Caudal, D., Francois, V., Lafoux, A., Ledevin, M., Anegon, I., Le Guiner, C., Larcher, T., Huchet, C., 2020. Characterization of brain dystrophins absence and impact in dystrophin-deficient Dmdmdx rat model. PloS One 15, e0230083

Chamberlain, J.S., Metzger, J., Reyes, M., Townsend, D., Faulkner, J.A., 2007. Dystrophin-deficient mdx mice display a reduced life span and are susceptible to spontaneous rhabdomyosarcoma. FASEB J 21, 2195-2204.

Dadgar, S., Wang, Z., Johnston, H., Kesari, A., Nagaraju, K., Chen, Y.W., Hill, D.A., Partridge, T.A., Giri, M., Freishtat, R.J., Nazarian, J., Xuan, J., Wang, Y., Hoffman, E.P., 2014. Asynchronous remodeling is a driver of failed regeneration in Duchenne muscular dystrophy. J Cell Biol 207, 139-158.

Dhindsa, J.S., McCall, A.L., Strickland, L.M., Fusco, A.F., Kahn, A.F., ElMallah, M.K., 2020. Motor axonopathies in a mouse model of Duchenne muscular dystrophy. Sci Rep 10, 8967.

Dobransky, T., Rylett, R.J., 2003. Functional regulation of choline acetyltransferase by phosphorylation. Neurochem Res 28, 537-542.

Duobles, T., Lima Tde, S., Levy Bde, F., Chadi, G., 2008. S100beta and fibroblast growth factor-2 are present in cultured Schwann cells and may exert paracrine actions on the peripheral nerve injury. Acta Cirurg 23, 555-560.

Goncalves, A.F., Dias, N.G., Moransard, M., Correia, R., Pereira, J.A., Witke, W., Suter, U., Relvas, J.B., 2010. Gelsolin is required for macrophage recruitment during remyelination of the peripheral nervous system. Glia 58, 706-715.

Grounds, M.D., 2008. Two-tiered hypotheses for Duchenne muscular dystrophy. Cell Mol Life Sci 65, 1621-1625.

Grounds MD, T.J., Al-Mshhdani BA, Duong MN, Radley-Crabb HG, Arthur PG., 2020. Biomarkers for Duchenne muscular dystrophy linked to myonecrosis, inflammation and oxidative stress. Dis. Model. Mech, 13(2)

Gumy, L.F., Katrukha, E.A., Kapitein, L.C., Hoogenraad, C.C., 2014. New insights into mRNA trafficking in axons. Dev Neurobiol 74, 233-244.

Haddix, S.G., Lee, Y.I., Kornegay, J.N., Thompson, W.J., 2018. Cycles of myofiber degeneration and regeneration lead to remodeling of the neuromuscular junction in two mammalian models of Duchenne muscular dystrophy. PloS One 13, e0205926.

Harriman, D.G., 1976. A comparison of the fine structure of motor end-plates in Duchenne dystrophy and in human neurogenic diseases. J Neurol Sci 28, 233-247.

Jessen, K.R., Mirsky, R., 1991. Schwann cell precursors and their development. Glia 4, 185-194.

Kornegay, J.N., 2017. The golden retriever model of Duchenne muscular dystrophy. Skeletal Muscle 7, 9.

Krishnan, V.S., Aartsma-Rus, A., Overzier, M., Lutz, C., Bogdanik, L., Grounds, M.D., 2020. Implications of increased S100beta and Tau5 proteins in dystrophic nerves of two mdx mouse models for Duchenne muscular dystrophy. Mol Cell Neurosci , 103484.

Krishnan, V.S., Shavlakadze, T., Grounds, M.D., Hodgetts, S.I., Harvey, A.R., 2018. Age-related loss of VGLUT1 excitatory but not VGAT inhibitory, immunoreactive terminals on motor neurons in spinal cords of old sarcopenic male mice. Biogerontology 19, 385-399.

Krishnan, V.S., White, Z., McMahon, C.D., Hodgetts, S.I., Fitzgerald, M., Shavlakadze, T., Harvey, A.R., Grounds, M.D., 2016. A neurogenic perspective of sarcopenia: time course study of sciatic nerves from aging mice. J Neurolpathol Exp Neurol 75, 464-478.

Krishnan, V.S., White, Z., Terrill, J.R., Hodgetts, S.I., Fitzgerald, M., Shavlakadze, T., Harvey, A.R., Grounds, M.D., 2017. Resistance wheel exercise from mid-life has minimal effect on sciatic nerves from old mice in which sarcopenia was prevented. Biogerontology 18, 769-790.

Lapidos, K.A., Kakkar, R., McNally, E.M., 2004. The dystrophin glycoprotein complex: signaling strength and integrity for the sarcolemma. Circ Res 94, 1023-1031.

Larcher, T., Lafoux, A., Tesson, L., et al 2014. Characterization of dystrophin deficient rats: a new model for Duchenne muscular dystrophy. PloS One 9, e110371.

Lee, G., Rook, S.L., 1992. Expression of tau protein in non-neuronal cells: microtubule binding and stabilization. J Cell Sci 102 (Pt 2), 227-237.

Lefaucheur, J.P., Pastoret, C., Sebille, A., 1995. Phenotype of dystrophinopathy in old mdx mice. Anat Rec 242, 70-76.

Lu, D.X., Huang, S.K., Carlson, B.M., 1997. Electron microscopic study of long-term denervated rat skeletal muscle. Anat Rec 248, 355-365.

Lyons, P.R., Slater, C.R., 1991. Structure and function of the neuromuscular junction in young adult mdx mice. J Neurocytol 20, 969-981.

Marques, M.J., Mendes, Z.T., Minatel, E., Santo Neto, H., 2005. Acetylcholine receptors and nerve terminal distribution at the neuromuscular junction of long-term regenerated muscle fibers. J Neurocytol 34, 387-396.

Marques, M.J., Taniguti, A.P., Minatel, E., Neto, H.S., 2007. Nerve terminal contributes to acetylcholine receptor organization at the dystrophic neuromuscular junction of mdx mice. Anat Rec 290, 181-187.

Minatel, E., Neto, H.S., Marques, M.J., 2003. Acetylcholine receptor distribution and synapse elimination at the developing neuromuscular junction of mdx mice. Muscle Nerve 28, 561-569.

Myeku, N., Figueiredo-Pereira, M.E., 2011. Dynamics of the degradation of ubiquitinated proteins by proteasomes and autophagy: association with sequestosome 1/p62. J Biol Chem 286, 22426-22440.

Painter, M.W., Brosius Lutz, A., Cheng, Y.C., et al 2014. Diminished Schwann cell repair responses underlie age-associated impaired axonal regeneration. Neuron 83, 331-343.

Pannerec, A., Springer, M., Migliavacca, E., Ireland, A., Piasecki, M., Karaz, S., Jacot, G., Metairon, S., Danenberg, E., Raymond, F., Descombes, P., McPhee, J.S., Feige, J.N., 2016. A robust neuromuscular system protects rat and human skeletal muscle from sarcopenia. Aging 8, 712-729.

Petrof, B.J., Shrager, J.B., Stedman, H.H., Kelly, A.M., Sweeney, H.L., 1993. Dystrophin protects the sarcolemma from stresses developed during muscle contraction. Proc Nat Acad Sci 90, 3710-3714.

Pratt, S.J.P., Valencia, A.P., Le, G.K., Shah, S.B., Lovering, R.M., 2015. Pre- and postsynaptic changes in the neuromuscular junction in dystrophic mice. Front Physiol 6, 252.

Shavlakadze, T., Soffe, Z., Anwari, T., Cozens, G., Grounds, M.D., 2013. Short-term feed deprivation rapidly induces the protein degradation pathway in skeletal muscles of young mice. J Nutri 143, 403-409.

Sheard, P.W., Bewick, G.S., Woolley, A.G., Shaw, J., Fisher, L., Fong, S.W., Duxson, M.J., 2010. Investigation of neuromuscular abnormalities in neurotrophin-3-deficient mice. Eur J Neurosci 31, 29-41.

Stedman, H.H., Sweeney, H.L., Shrager, J.B., Maguire, H.C., Panettieri, R.A., Petrof, B., Narusawa, M., Leferovich, J.M., Sladky, J.T., Kelly, A.M., 1991. The mdx mouse diaphragm reproduces the degenerative changes of Duchenne muscular dystrophy. Nature 352, 536-539.

Tanaka, J., Sobue, K., 1994. Localization and characterization of gelsolin in nervous tissues: gelsolin is specifically enriched in myelin-forming cells. J Neurosci 14, 1038-1052.

Torres, L.F., Duchen, L.W., 1987. The mutant mdx: inherited myopathy in the mouse. Morphological studies of nerves, muscles and end-plates. Brain 110 (Pt 2), 269-299.

Toussaint, M., Davidson, Z., Bouvoie, V., Evenepoel, N., Haan, J., Soudon, P., 2016. Dysphagia in Duchenne muscular dystrophy: practical recommendations to guide management. Disabil Rehabil 38, 2052-2062.

Triolo, D., Dina, G., Taveggia, C., Vaccari, I., Porrello, E., Rivellini, C., Domi, T., La Marca, R., Cerri, F., Bolino, A., Quattrini, A., Previtali, S.C., 2012. Vimentin regulates peripheral nerve myelination. Development 139, 1359-1367.

van der Pijl, E.M., van Putten, M., Niks, E.H., Verschuuren, J.J., Aartsma-Rus, A., Plomp, J.J., 2016. Characterization of neuromuscular synapse function abnormalities in multiple Duchenne muscular dystrophy mouse models. Eur J Neurosci 43, 1623-1635.

van Putten, M., Lloyd, E.M., de Greef, J.C., Raz, V., Willmann, R., Grounds, M.D., 2020. Mouse models for muscular dystrophies: an overview. Dis Model Mech 13.

Vandesompele, J., De Preter, K., Pattyn, F., Poppe, B., Van Roy, N., De Paepe, A., Speleman, F., 2002. Accurate normalization of real-time quantitative RT-PCR data by geometric averaging of multiple internal control genes. Genome Biol 3, 1-11.

Verhaart, I.E.C., Aartsma-Rus, A., 2019. Therapeutic developments for Duchenne muscular dystrophy. Nat Rev Neurol 15, 373-386.

Wells, D.J., 2018. Tracking progress: an update on animal models for Duchenne muscular dystrophy. Dis Model Mech 11.

Willmann, R., Possekel, S., Dubach-Powell, J., Meier, T., Ruegg, M.A., 2009. Mammalian animal models for Duchenne muscular dystrophy. Neuromuscul Disord 19, 241-249.

Yuan, A., Rao, M.V., Veeranna, Nixon, R.A., 2012. Neurofilaments at a glance. J Cell Sci 125, 3257-3263.

Journal Pre-proof

AUTHOR CONTRIBUTIONS

Krishnan VS: Data curation, Formal analysis, Investigation, Methodology, Supervision, Software, Visualization, Validation, Roles/Writing original draft, Writing-review and editing

Thanigaiarasu LP: Data Curation, Formal analysis, Investigation, Software, Visualization, Writing-review and editing

White R: Investigation, Writing-review and editing

Crew R: Investigation, Writing-review and editing

Larcher T: Resources, Writing –review and editing

Le Guiner C: Resources, Writing-review and editing

Grounds MD: Conceptualization, Resources, Funding acquisition, Project administration, Supervision, Roles/Writing original draft, Writing-review and editing

Journal Pre-proof

HIGHLIGHTS

- Quantification of proteins in dystrophic nerves from the Dmd^{mdx} rat model of DMD
- S100β and Tau5 proteins increase in sciatic nerves of Dmd^{mdx} rats aged 8 months
- Supports severity of myonecrosis and ongoing dystropathology in the rat model of DMD
- Less pronounced neuronal changes in classic *mdx* mice at 9 months
- Suggests Dmd^{mdx} rats as a more consistent model compared to *mdx* mice

Journal Pre-proof

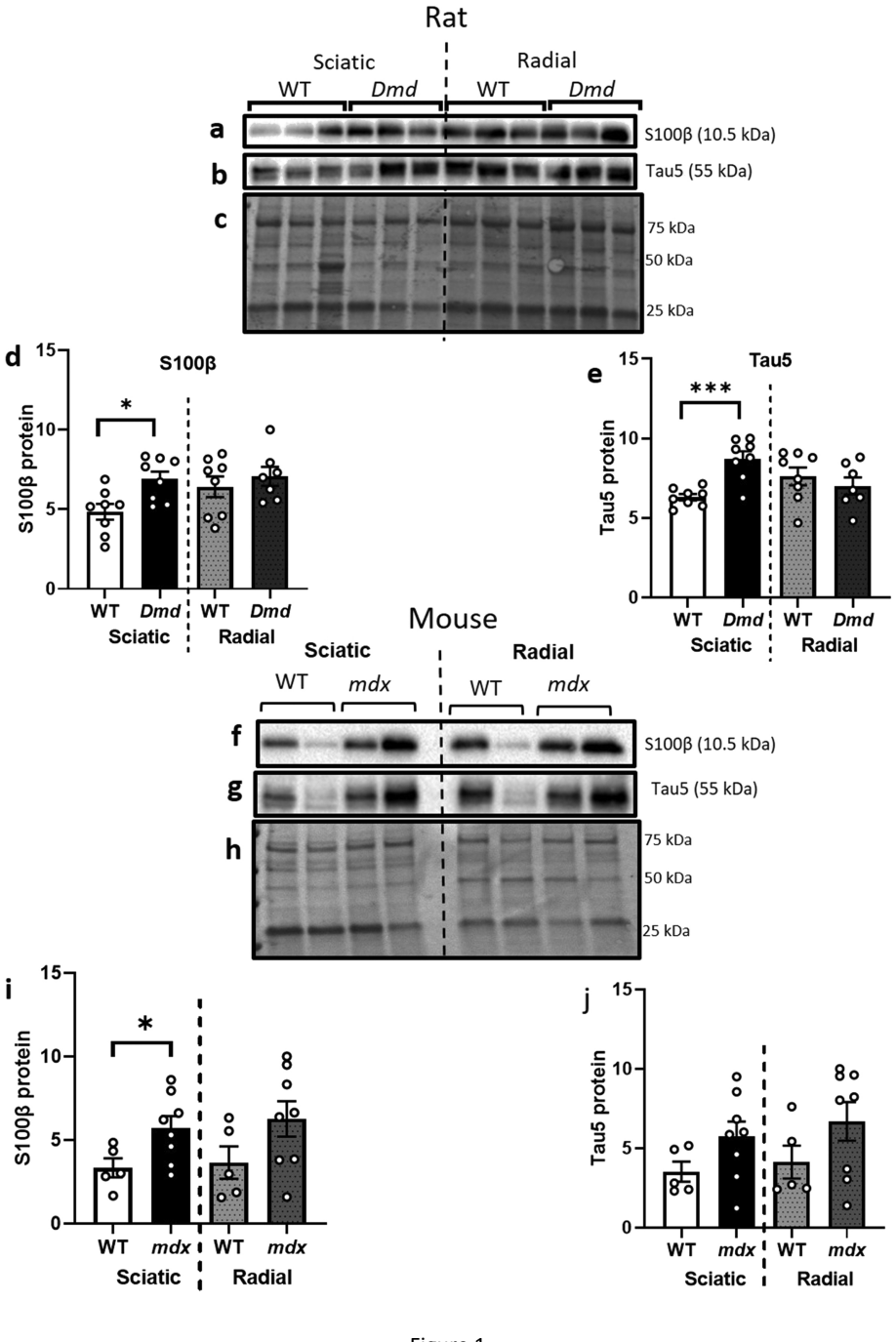
Rat
Sciatic
Radial
WT
Dmd
WT
Dmd
a
S100β (10.5 kDa)
b
Tau5 (55 kDa)
c
75 kDa
50 kDa
25 kDa
d
S100β
S100β protein
*
WT
Dmd
WT
Dmd
Sciatic
Radial
e
Tau5
Tau5 protein
***
WT
Dmd
WT
Dmd
Sciatic
Radial
Mouse
Sciatic
Radial
WT
mdx
WT
mdx
f
S100β (10.5 kDa)
g
Tau5 (55 kDa)
h
75 kDa
50 kDa
25 kDa
i
S100β protein
*
WT
mdx
WT
mdx
Sciatic
Radial
j
Tau5 protein
WT
mdx
WT
mdx
Sciatic
Radial

Figure 1

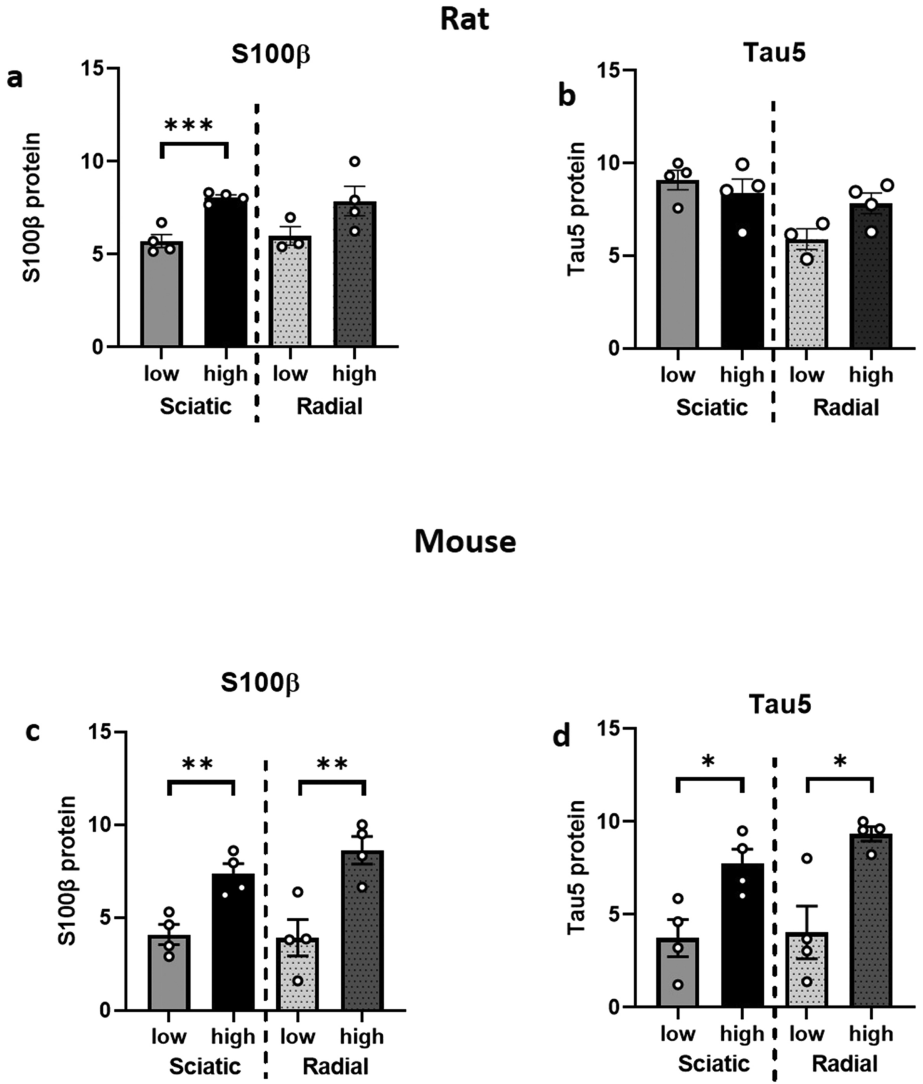
Rat
a
S100β
S100β protein
15
10
5
0
***
low
high
low
high
Sciatic
Radial
b
Tau5
Tau5 protein
15
10
5
0
low
high
low
high
Sciatic
Radial
Mouse
c
S100β
S100β protein
15
10
5
0
**
**
low
high
low
high
Sciatic
Radial
d
Tau5
Tau5 protein
15
10
5
0
*
*
low
high
low
high
Sciatic
Radial

Figure 2

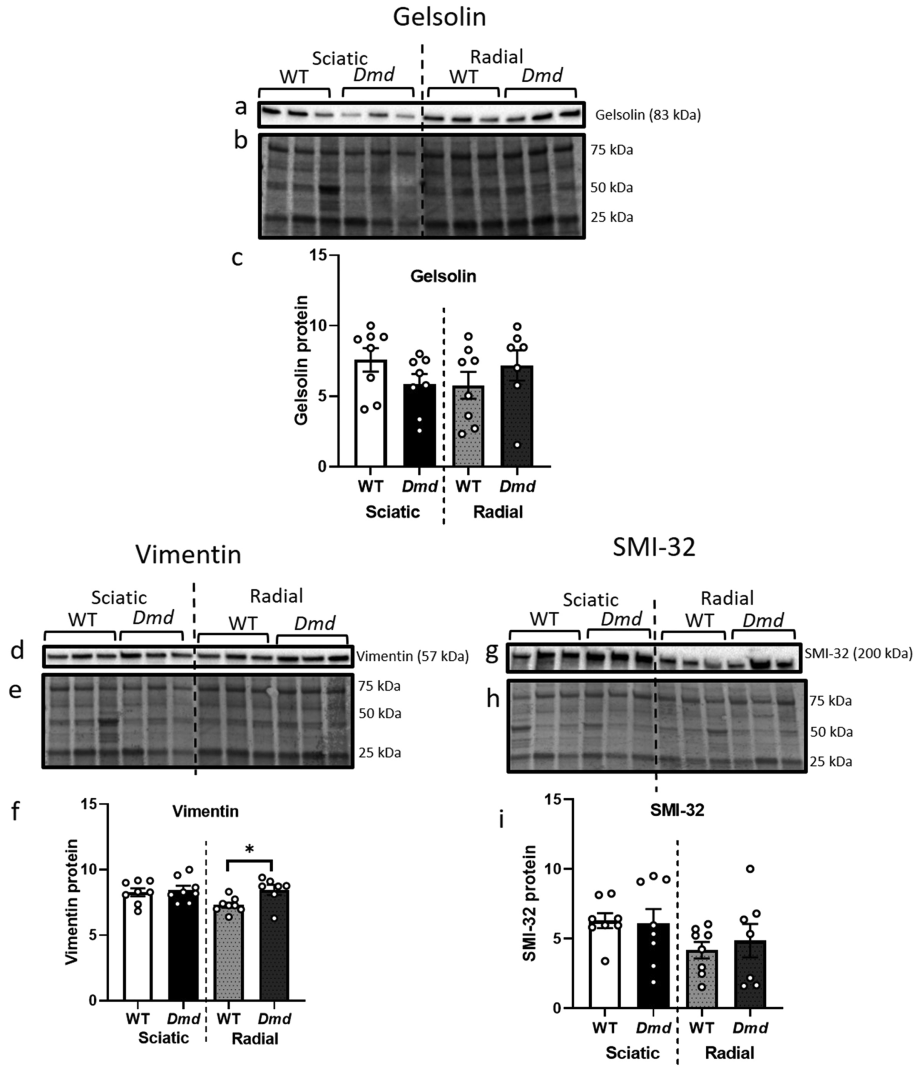
Gelsolin
Sciatic
Radial
WT
Dmd
WT
Dmd
a
Gelsolin (83 kDa)
b
75 kDa
50 kDa
25 kDa
c
Gelsolin
Gelsolin protein
15
10
5
0
WT
Dmd
WT
Dmd
Sciatic
Radial
Vimentin
Sciatic
Radial
WT
Dmd
WT
Dmd
d
Vimentin (57 kDa)
e
75 kDa
50 kDa
25 kDa
f
Vimentin
Vimentin protein
*
15
10
5
0
WT
Dmd
WT
Dmd
Sciatic
Radial
SMI-32
Sciatic
Radial
WT
Dmd
WT
Dmd
g
SMI-32 (200 kDa)
h
75 kDa
50 kDa
25 kDa
i
SMI-32
SMI-32 protein
15
10
5
0
WT
Dmd
WT
Dmd
Sciatic
Radial

Figure 3

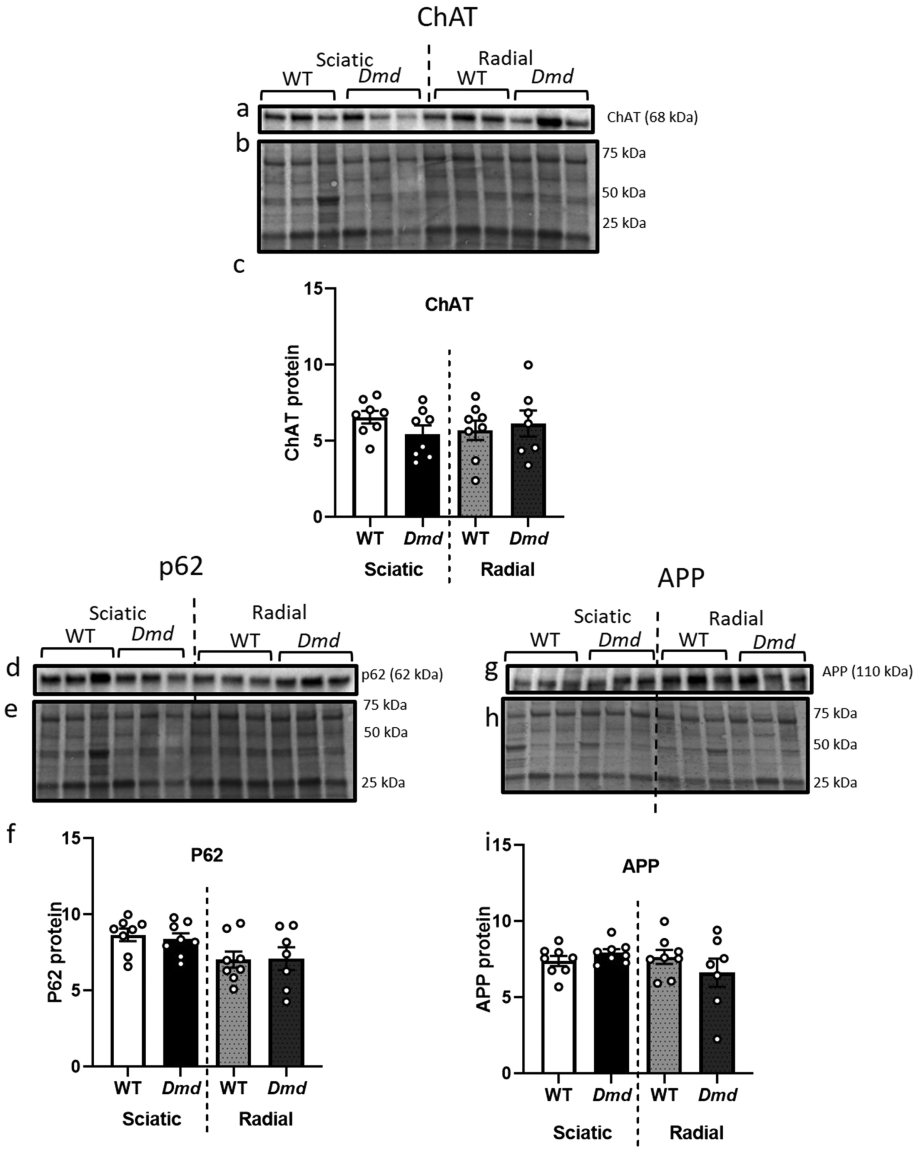
ChAT
Sciatic
Radial
WT
Dmd
WT
Dmd
a
ChAT (68 kDa)
b
75 kDa
50 kDa
25 kDa
c
ChAT
ChAT protein
15
10
5
0
WT
Dmd
WT
Dmd
Sciatic
Radial
p62
Sciatic
Radial
WT
Dmd
WT
Dmd
d
p62 (62 kDa)
e
75 kDa
50 kDa
25 kDa
APP
Sciatic
Radial
WT
Dmd
WT
Dmd
g
APP (110 kDa)
h
75 kDa
50 kDa
25 kDa
f
P62
P62 protein
15
10
5
0
WT
Dmd
WT
Dmd
Sciatic
Radial
i
APP
APP protein
15
10
5
0
WT
Dmd
WT
Dmd
Sciatic
Radial

Figure 4

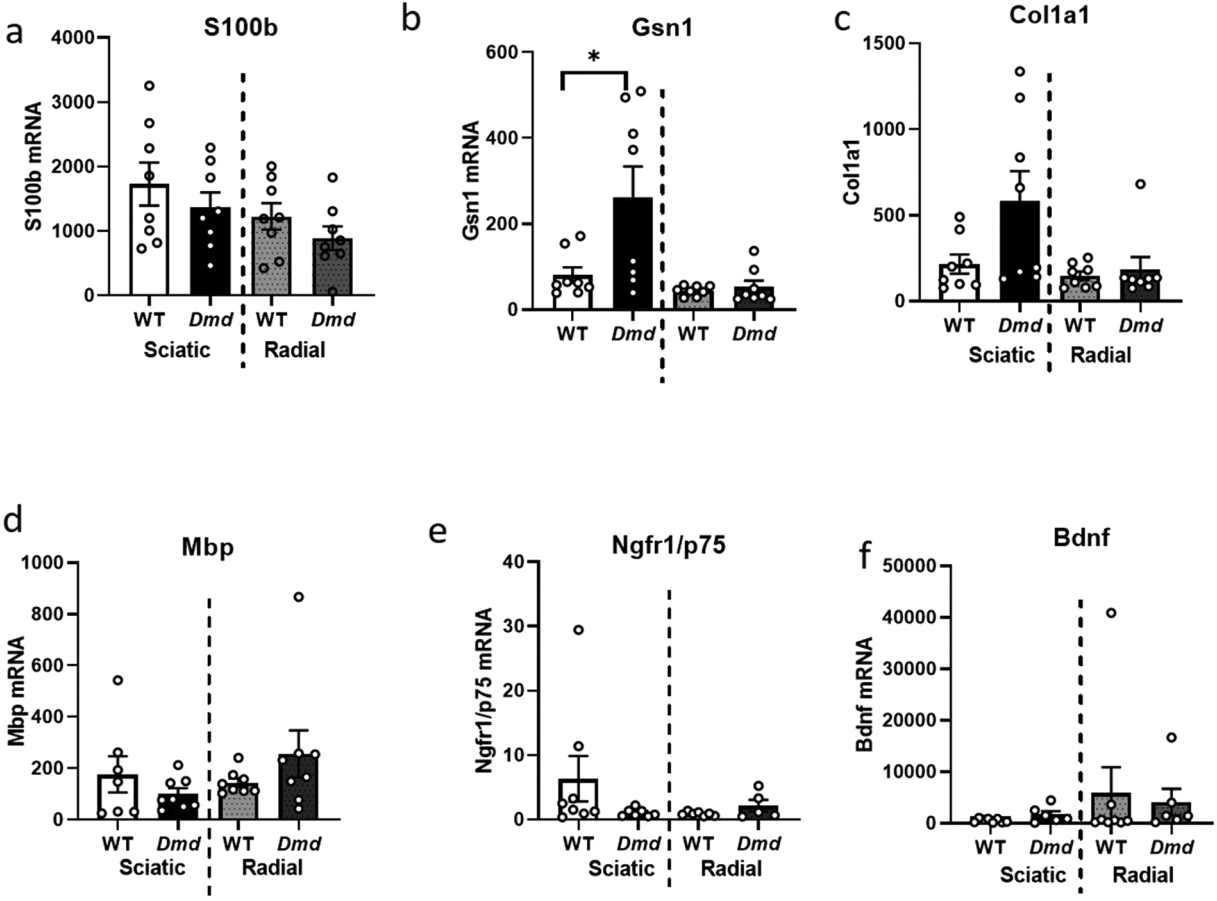
a
S100b
S100b mRNA
4000
3000
2000
1000
0
WT
Dmd
WT
Dmd
Sciatic
Radial
b
Gsn1
Gsn1 mRNA
600
400
200
0
*
WT
Dmd
WT
Dmd
c
Col1a1
Col1a1
1500
1000
500
0
WT
Dmd
WT
Dmd
Sciatic
Radial
d
Mbp
Mbp mRNA
1000
800
600
400
200
0
WT
Dmd
WT
Dmd
Sciatic
Radial
e
Ngfr1/p75
Ngfr1/p75 mRNA
40
30
20
10
0
WT
Dmd
WT
Dmd
Sciatic
Radial
f
Bdnf
Bdnf mRNA
50000
40000
30000
20000
10000
0
WT
Dmd
WT
Dmd
Sciatic
Radial

Figure 5

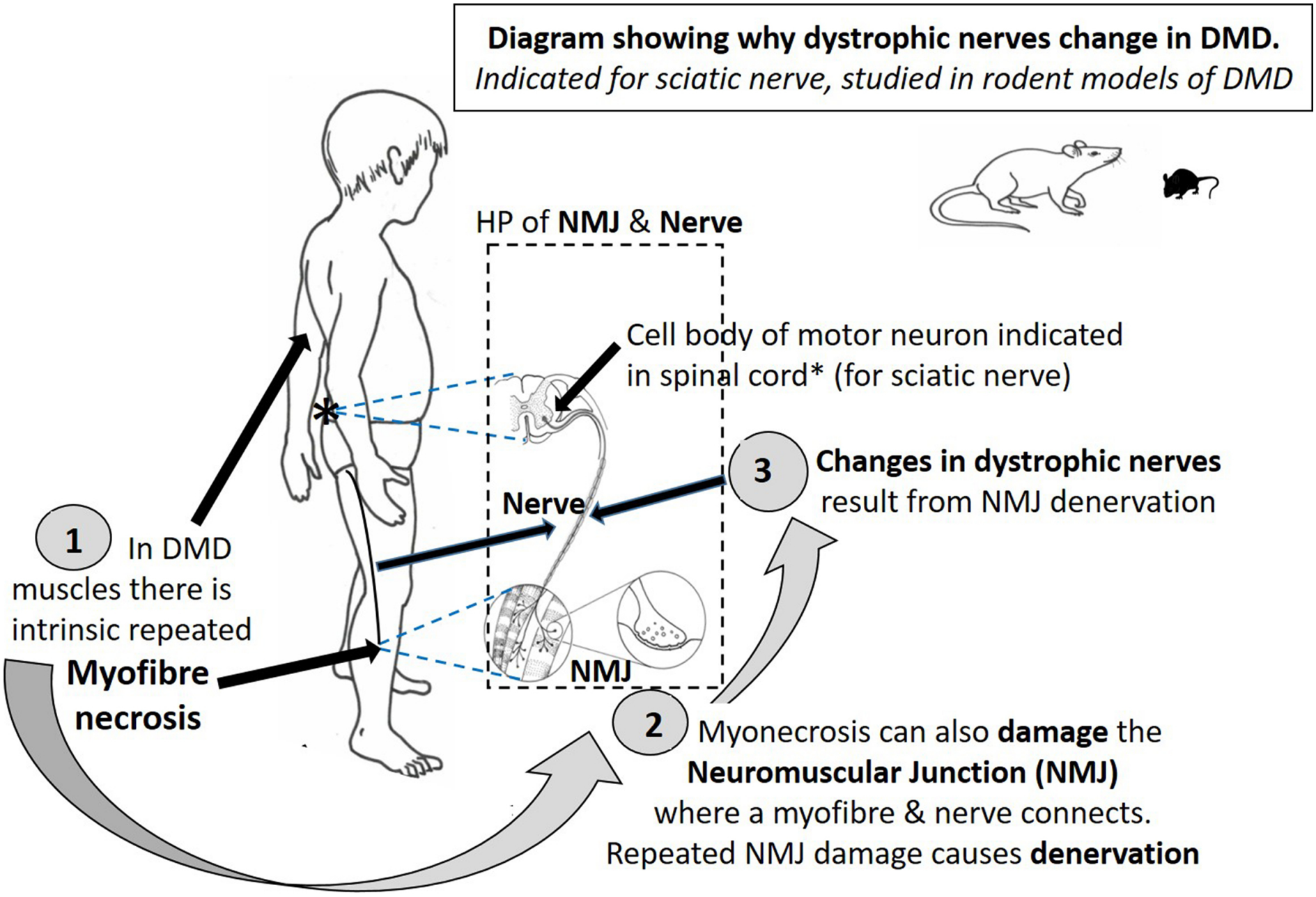
Diagram showing why dystrophic nerves change in DMD.
Indicated for sciatic nerve, studied in rodent models of DMD
HP of NMJ & Nerve
Cell body of motor neuron indicated in spinal cord* (for sciatic nerve)
3
Changes in dystrophic nerves result from NMJ denervation
Nerve
1
In DMD muscles there is intrinsic repeated
Myofibre necrosis
NMJ
2
Myonecrosis can also damage the Neuromuscular Junction (NMJ) where a myofibre & nerve connects. Repeated NMJ damage causes denervation

Figure 6